UNIVERSITÀ DEGLI STUDI DI TORINO

Elena Morra,Elio Giamello,Mario Chiesa. Probing the Redox Chemistry of Titanium Silicalite-1: Formation of Tetrahedral Ti3+Centers by Reaction with Triethylaluminum. CHEMISTRY-A EUROPEAN JOURNAL, 20, 2014: 7381-7388.
DOI: 10.1002/chem.201304139

Probing the Redox Chemistry of Ti Silicalite-1. Formation of Tetrahedral Ti^{3+} Centers by Reaction with Triethylaluminium.

Elena Morra, Elio Giamello and Mario Chiesa*[a.b]

Abstract: Transition metal ions with open-shell configurations hold promises in the development of novel coordination chemistry and potentially unprecedented redox catalysis. In the present work we generate framework substituted Ti^{3+} ions with tetrahedral coordination by reductive activation of Titanium Silicalite-1 with triethylaluminium, an indispensable co-catalyst for heterogeneous Ziegler-Natta polymerization catalysts. Continuous wave and pulse Electron Paramagnetic Resonance methods are applied to unravel details on the local environment of the reduced transition metal ions, which are shown to be part of the silica framework by detection of ^{29}Si hyperfine interactions. The chemical accessibility of the reduced sites is probed using ammonia as probe molecule. Evidence is found for the coordination of a single ammonia molecule. Comparison to similar systems such as TiAlPO-5 reveals clear differences in the coordination chemistry of the reduced Ti sites in the two solids, which may be understood considering the different electronic properties of the solid frameworks.

Keywords: Titanium Silicalite, • Titanium (III) • ESR • Ziegler-Natta catalysts Heterogeneous catalysis

Introduction

The incorporation of transition metal ions (TMI) in the framework of micro and mesoporous materials generates isolated sites that often lack structural precedent in molecular chemistry. These active metal centers give rise to a formidable variety of processes and exert different functionalities, which are critically modulated by the nature of the surrounding ligands, the local coordination geometry and the specific oxidation states.

A prototypical example is the insertion of Ti ions in the frame of silicalite to generate Titanium silicalite-1 (TS-1) [1], one of the most extensively used catalysts for the selective oxidation of hydrocarbons, an essential pathway for the functionalization of petroleum based feed stocks.

The distinctive feature of TS-1 is the presence of isolated Ti ions forced to assume an unusual tetrahedral coordination by insertion in the rigid framework of the solid. Indeed it is this open coordination that primes the diluted metal centers for the remarkable inner-sphere redox reactivity of TS-1. Ti^{4+} sites in TS-1 have been the object of intense and detailed characterization from both the experimental and theoretical point of view [2-7] and consensus has been reached in establishing that Ti is preferentially located inside a tetrapodal structure [8]. On the other hand, much less is known concerning the redox chemistry of TS-1 and in particular on the structural details of reduced Ti^{3+} species generated in the framework. The generation and characterization of tetrahedral Ti^{3+} species in open frame materials is to a large extent unexplored, although the importance of such an open shell configuration in catalysis is well recognized. Electron Paramagnetic Resonance (EPR) studies have been reported in the past to probe the nature of Ti^{3+} species in TS-1, however clear evidence of tetrahedrally coordinated Ti^{3+} ions was only obtained upon irradiation of the solid under ionizing radiations, while chemical reduction led to spectra amenable to distorted octahedral coordination [9], likely due to reduction of extra framework TiO_2 impurity phases.

The reactivity of open shell Ti^{3+} compounds in catalysis is at the heart of important processes such as olefins polymerization in Ziegler Natta catalysis; however compounds featuring these reduced Ti states are relatively rare. Recently Ti^{3+}-MOF materials have been synthesized, which display interesting reactive properties [10]. The unpaired spin density and highly reducing nature of Ti^{3+} make these ions capable of promoting selective radical-type transformations as well as exerting important effects in the selectivity through the subtle participation of the Singly Occupied Molecular Orbital (SOMO) to the reaction [11]. It is worth noting that such a role of the SOMO is at the basis of so called SOMO organo-catalysis [12], an entire new research area, which remains to a large extent unexplored in heterogeneous catalysis.

The focus of this work is thus on the redox properties of framework Ti^{4+} ions in TS-1 with emphasis on the properties of Ti^{3+} framework centers generated by chemical reaction with alkyl aluminium compounds. In particular we use triethylaluminium (TEA) vapors to reduce framework isolated Ti centers and explore their structure and reactivity by means of continuous wave (CW) and pulse EPR techniques.

Alkyl aluminium compounds are indispensable activating agents for olefin polymerization with Ziegler-Natta catalysts, where formation of the active sites is generally accepted to proceed by alkylation and reduction of the titanium species in the catalyst during the activation

reaction. Alkyl aluminium compounds are also prototypical precursors to the industrially important methyl aluminoxane co-catalysts for olefin polymerization and recently have been used to introduce well-defined extra framework aluminium ions in zeolite materials [13-15].

The isolated Ti centers in TS-1 represent thus interesting candidates to explore the interaction of a typical catalyst activator such as TEA and its redox activity towards a silica based zeolite incorporating potentially active catalytic sites. To elucidate the result of such a redox reactivity we employ CW and pulse EPR techniques focusing on HYSCORE spectroscopy, which enables to detect the hyperfine interaction of the unpaired electron localized on the Ti^{3+} ions formed upon reaction, with magnetically active nuclei in the surrounding, including natural abundant framework ^{29}Si and ^{14}N of adsorbed ammonia molecules.

Results and Discussion

3.1. EPR spectra of Ti^{3+} in reduced TS-1

Calcined and dehydrated TS-1 samples do not show any EPR signal at 77 K as expected for Ti species in the form of diamagnetic Ti^{4+}. Attempts to reduce the sample by heating under hydrogen atmosphere, as done by some of us in the case of TiAlPO materials [16], led to very weak and ill resolved spectra indicating a lower reducibility of Ti in TS-1 with respect to TiAlPO under the same conditions.

Upon contacting the solid with TEA vapors an intense EPR spectrum with pseudo-axial symmetry is given rise, which is reported in Figure 1a. The spectral intensity is found to depend on the contact time between the sample and the TEA vapors over a large time span (days). This is primarily due to two factors: 1) the dimerization equilibrium of TEA, which makes inactive dimeric species to be largely predominant in the condensed phase (99.92% at 298 K) [17]; 2) the slow diffusion of TEA inside the pores of the solid. For these reasons we followed the reaction only from a qualitative point of view.

The spectrum, although similar to the one previously reported by Kevan [9] and obtained by low temperature γ irradiation of the solid shows a much higher resolution and absence of matrix defect signals with respect to the irradiated system of ref. [9], allowing for a precise determination of the **g** tensor by means of computer simulation (Figure 1 and Table 1). The simulation analysis shows that the spectral profile is dominated by a species (species 1) with slightly rhombic **g** tensor (g_1 = 1.922, g_2 = 1.939, g_3 = 1.9897). The best fit of the experimental pattern was however obtained including a second species (species 2 in Table 1) with maximum abundance of 10% as estimated from the computer simulation. From the estimated **g** tensor values this species may be assigned to Ti^{3+} species with a different environment, either due to interactions with TEA residuals or to a non regular framework site position. We remark however, that given the low abundance of this species and the nearly complete overlapping with the dominant signal, the error in the determination of the *g* values is rather large and we will not consider this further. The observed signal for Ti^{3+} in TS-1 is closely similar to the signal observed in TiAlPO [16] and TiMCM-41 [18] and indicates similar crystalline symmetry for this ion in these materials. The *g* factors are also in line with those reported for Ti^{3+} defect centers, where Ti^{3+} ions substitute for the tetrahedral Si^{4+} site of beryl crystals [19].

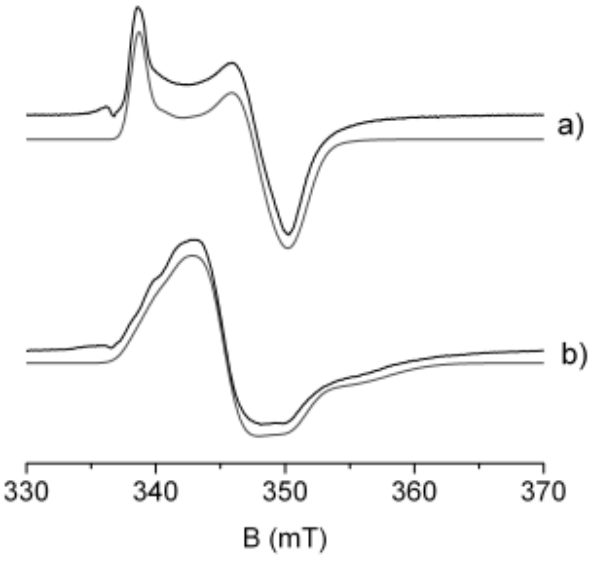

Figure 1. Experimental (black line) and simulated (grey line) CW-EPR spectra of reduced TS-1(a) and reduced TS-1 contacted with NH_3 (b). The spectra were recorded at 77 K.

The *g* factor components of Ti^{3+} ($3d^1$, ^2D) species are strongly dependent on the local symmetry felt by the cation. When Ti^{3+} is subjected to a perfect cubic crystalline field from tetrahedral or octahedral coordination, its 5-fold orbital degeneracy is split into two and three degenerate levels. In a tetrahedral field the doublet has lower energy, whereas in an octahedral field the reverse is true. In both cases a distortion from perfect cubic symmetry is expected for a $3d^1$ system in order to explain the experimentally observed anisotropy of the EPR

signal. In the classical crystal-field theory, the EPR parameters are explained by using the perturbation formulas based on the one-spin-orbit (SO)-parameter model [20] or, to a more refined level of theory, considering the two SO parameter model [21]. This model has been used to calculate theoretical *g* values, within the rhombic symmetry approximation, in the case of the tetrahedral Ti^{3+} defect center in beryl crystal.[22] Here we limit ourselves to consider that in the simple case of an axial symmetry the theoretical expressions for *g* values calculated to first order are

Table 1. *g* matrix components for Ti^{3+} species at tetrahedral sites of different materials and in the presence of ammonia.

System	Species	Abundance (%)	g_1	g_2	g_3	Ref.
TS-1	1	90	1.922 ± 0.001	1.939 ± 0.001	1.9897 ± 0.0002	This work
	2	10	1.981 ± 0.002	1.960 ± 0.005	1.91 ± 0.01	
γ-irradiated TS-1			1.906	1.906	1.970	[9]
TiMCM-41			1.901	1.901	1.971	[18]
TiAlPO-5	1	65	1.898 ± 0.005	1.918 ± 0.005	1.991 ± 0.002	[16]
	2	35	1.90 ± 0.01	1.90 ± 0.01	1.969 ± 0.002	
Ti^{3+} at the tetrahedral Si^{4+} site of beryl crystals			1.866	1.907	1.988	[19]
TS-1 / NH_3	1	60	1.965 ± 0.005	1.949 ± 0.001	1.90 ± 0.01	This work
	2	20	1.981 ± 0.002	1.970 ± 0.01	1.91 ± 0.02	
	3	20	1.922 ± 0.005	1.939 ± 0.005	1.990 ± 0.001	
TiMCM-41 / NH_3			1.961	1.946	1.920	[18]
TiAlPO-5 / NH_3			1.946 ± 0.001	1.913 ± 0.006	1.895 ± 0.006	[26]

[23] $g_{\parallel} \approx g_e$ and $g_{\perp} \approx g_e - 6\lambda/\Delta$, where g_e is the free electron *g* value (2.0023), Δ is the energy gap between the ground state and excited levels and λ the Ti spin orbit coupling constant (≈ 154 cm^{-1}) [24]. Substituting the *g* experimental values in the above equations Δ can be estimated to be of the order of 12500 cm^{-1}, which fits relatively well, given the inherent approximation, with values reported for *d-d* transitions of tetrahedral Ti^{3+} [25]. The chemical accessibility of the formed Ti^{3+} species can be tested by adsorption of suitable molecules such as NH_3. Adsorption of NH_3 at the active EPR site is expected to lead to a modification of the local crystal field experienced by the metal cation and this, in turn, is expected to have profound influence on the *g* factors of the EPR spectrum. Indeed upon adsorption of ammonia the features of the spectrum reported in Figure 1a drastically change, giving rise to a new spectrum (Figure 1b) dominated by a species whose *g* components are g_1 = 1.965, g_2 = 1.949, and g_3 = 1.90 (Table 1) typical for Ti^{3+} species characterized by a distorted octahedral field. In agreement with the slight heterogeneity of the EPR spectrum of reduced TS-1, also in the case of ammonia adsorption, more species were needed to correctly reproduce the experimental spectral pattern. In particular, species 2 is characterized by *g* factors that are still consistent with a distorted octahedral symmetry, while species 3 indicates that a fraction of the original tetrahedral Ti^{3+} centers remained unreacted under these conditions. The observed *g* factors are consistent with those reported for ammonia adsorbed on Ti^{3+} species in TiMCM-41 [18] and TiAlPO-5 [26] systems. Comparison with this latter system is particularly interesting as in both cases Ti^{3+} species are formed at tetrahedral sites, which however differ in their chemical nature, being the network constituted in one case by SiO_4^{4-} tetrahedra and in the other case by strictly alternating AlO_4^{5-} and PO_4^{3-} groups. We will dwell upon this comparison after analyzing the local environment of Ti^{3+} species prior and after ammonia adsorption by means of HYSCORE spectroscopy.

3.2. HYSCORE spectra of reduced TS-1

The *g* factor analysis of the CW-EPR spectrum thus strongly indicates the formation of framework Ti^{3+} ions in tetrahedral coordination upon reaction of the dehydrated sample with TEA vapors. In order to confirm this analysis and to ascertain the local coordination environment of the formed Ti^{3+} species, HYSCORE experiments have been performed. Figure 2 shows the HYSCORE spectrum of the TS-1 reduced sample taken at the observer position corresponding to the turning point of the EPR spectrum (see arrow in the inset).

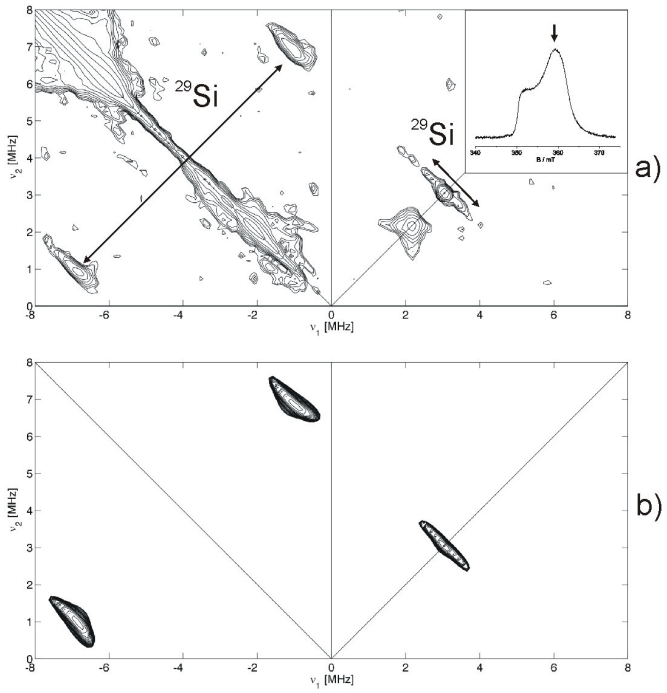

Figure 2. a) Experimental and b) simulated ^{29}Si HYSCORE spectra of reduced TS-1 taken at observer position 359.5 mT corresponding to the arrow in the inset . Two τ *values* (192 ns and 224 ns) are summed together after Fourier transform in both the experimental and simulated spectra. The simulation was performed considering a three spin system (S=1/2, I=1/2, I=1/2). Spectra taken at other observer positions are reported as Supporting information.

Table 2**.** ^{29}Si hyperfine coupling constants. All values are in MHz.

System	A_1	A_2	A_3	Ref.
TS-1	-6.8 ± 0.2	-7.1 ± 0.2	-10.0 ± 0.2	This work
	0.3 ± 0.3	0.3 ± 0.3	-1.6 ± 0.4	
TCV	-6.0 ± 0.3	-8 ± 1	-9.4 ± 0.3	[27]
	0.3 ± 0.4	0.3 ± 0.4	-1.6 ± 0.2	

The spectrum is characterized by the presence in the (-,+) quadrant of a pair of cross peaks centered at about (-0.92, +6.62) MHz and (-6.62, +0.92) MHz which are unambiguously assigned to (relatively) strongly coupled ^{29}Si in the surrounding of the Ti^{3+} center. The signal intensity is relatively low according to the low natural abundance of ^{29}Si (4.67%). The elongated shape of the cross peaks indicates a relatively large anisotropy. A second set of ^{29}Si interactions is observed in the (+,+) quadrant, where a ridge with maximum extension of approximately 2.0 MHz is centered at the ^{29}Si Larmor frequency. The hyperfine coupling constant parameters were extracted by means of computer simulation of the experimental spectrum (Figure 2) and are listed in Table 2, where the signs were chosen based on the point dipolar approximation and considering that $g_n(^{29}Si) < 0$. We remark that given the low intensity, poor orientational selectivity and overlap with ^{29}Si matrix signals the hyperfine coupling constants for the weakly coupled Si in the (+,+) quadrant, in particular, are affected by relatively large errors (Table 2).

The values for both set of nuclei compare nicely with those reported by Zamani et al. [27] in the case of VO^{2+} groups incorporated in mesoporous silica materials (TCV in Table 2) and together with the g factors of the CW-EPR spectrum (characteristic of a local tetrahedral symmetry) provide unique and direct evidence for the framework incorporation of the formed Ti^{3+} species. We remark that this result is non trivial as, although the starting TS-1 material features framework incorporated Ti^{4+} ions, chemical reduction to Ti^{3+} not necessarily implies that the reduced species preserves its framework nature and local coordination symmetry.

The hyperfine tensors reported in Table 2 can be decomposed in the usual way in the isotropic (Fermi contact) A_{iso} = -8.0 MHz and -0.33 MHz and anisotropic (dipolar) tensors [+1.2 +0.9 -2.0] MHz and [+0.63 +0.63 -1.2] MHz for the strongly and weakly coupled ^{29}Si respectively.

The strongly coupled ^{29}Si interaction is dominated by the Fermi contact term. The origin of this fairly large isotropic interaction can be rationalized considering a spin density transfer through the directly coordinated oxygen ions via a through-bond mechanism. The isotropic constant is determined mainly by the unpaired spin density in the 3*s* orbital of the silicon atoms and is proportional to the value of a_0 = -3995.33 MHz, which is computed for unit spin density in this orbital [28]. Including a correction for departure of the g value ($g_{iso}[Ti^{3+}$/TS-1] = 1.950) from the free electron value (g_e = 2.0023) the spin population in the Si 3*s* orbital can be estimated from the following equation:

$$\rho_{Si(3s)} = \frac{A_{iso}}{a_0}\frac{g_e}{g_{iso}} \quad (1)$$

to be approximately 0.20% and 0.008% for the two cases. As discussed by different Authors in the case of similar systems [16,29], the amount of spin density transfer is expected to depend markedly on bond angle and distance of the fragment Ti-O-Si, making the Fermi contact term a sensitive structural probe. Comparison can be set to the case of framework substituted Ti^{3+} ions in AlPO-5 materials. In that case Ti^{3+} species experience the same tetrahedral field as testified by the similarity of the *g* matrix components (Table 1) but the nearest cations are ^{31}P instead of ^{29}Si. Also in that case the ^{31}P hyperfine interaction is dominated by the isotropic term, which varies from a maximum of 19.3 MHz to a minimum of 1.7 MHz. Considering the value of a_0 = 10201.44 MHz for unit spin density on the ^{31}P 3*s* orbital [28] and $g_{iso}[Ti^{3+}/TiAlPO\text{-}5]$ = 1.935 [16], the corresponding spin density in the P 3*s* orbital is ≈ 0.20% and 0.017% in line with the present results and those obtained for VO^{2+} species in mesoporous silica materials [27]

The anisotropic coupling is the result of two factors: dipole-dipole (through space) coupling and indirect (through bond) spin transfer. The first term is mainly dictated by the Ti-Si distance, while the second induces a spin density transfer on the Si 3*p* orbitals, which is the origin of the slight departure from axiality of the dipolar tensor for the strongly coupled ^{29}Si. We notice that as in the previous case this spin density transfer mechanism is strongly dependent on the bonding geometry of the Ti-O-Si fragment, however, being the value for unit electron occupancy of a 3*p* orbital of Si approximately 16 times less the value obtained for a 3*s* orbital, this parameter is a less sensitive structural probe. Assuming a simple point-dipolar approximation (Eq. 2), the distance of the ^{29}Si nucleus to the Ti^{3+} center can be estimated as being 0.25 nm and 0.29 nm for the strongly and weakly coupled ^{29}Si respectively. These values coincide with those reported by ref [27] for V-Si in VS-1 and are approximately 20% and 10% smaller than the Ti-Si distance in TS-1 obtained from EXAFS and theoretical calculations [30]. This discrepancy clearly indicates that the simple point-dipolar approximation does not hold and small spin density transfer in the Si p-orbital(s) (which will depend on the Ti-O-Si bond angle) will need to be considered. This derived distances, should be thus only taken as rough estimates. Based on this analysis we can then rationalize the observation of two types of ^{29}Si hyperfine interactions in terms of framework incorporation of the Ti^{3+} species, whereby the difference in the hyperfine couplings can be naturally explained considering the different bonding geometry (length and angle) of the Ti-O-Si fragments. We notice that in the case of TiAlPO-5 four distinct hyperfine couplings to the coordinated ^{31}P units were observed, while in our case, despite the four-fold coordination (Scheme 1), we only see two distinct ^{29}Si couplings. This may be explained considering that nearly equivalent ^{29}Si may be present, which cannot be distinguished in the experiment. Also, being the value of the isotropic component for unit occupancy of the ^{29}Si 3*s* orbital nearly three times smaller than that of ^{31}P, the sensitivity of this parameter to structural variations is correspondingly lower in the case of ^{29}Si. It remains however, that the observation of these ^{29}Si hyperfine interactions provides direct and unambiguous evidence for incorporation of the transition metal ion into the siliceous framework, providing yet another example of the power of hyperfine EPR techniques to probe the isomorphous framework substitution of (paramagnetic) transition metal ions in porous heterogeneous catalysts. [27, 31, 32]

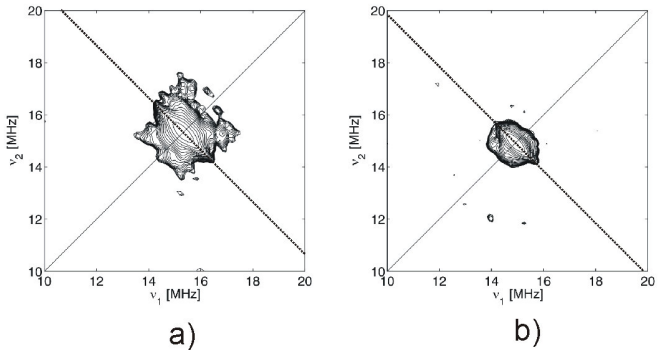

Figure 3. Experimental ^1H HYSCORE spectra of reduced TS-1 taken at observer positions a) 359.5 mT and b) 350.2 mT corresponding to the turning points of the EPR spectrum. The dotted lines indicate the ^1H Larmor frequency at the two frequencies. The HYSCORE spectra taken at three τ values (96, 192 and 224 ns) are summed together after Fourier transform. The simulations of the spectra are reported as Supporting Information.

In addition to signals associated to ^{29}Si, HYSCORE spectra of reduced TS-1, also show, centered at the ^1H nuclear Larmor frequency, a small ridge due to the superhyperfine interaction between Ti^{3+} and a proton, amenable to the TEA alkyl residual groups. The maximum ridge extension is of the order of 2.5 MHz (Figure 3). The full hyperfine coupling tensor was obtained by simulation of the experimental spectra at two magnetic field settings corresponding to the turning points of the EPR powder spectrum. The following parameters were obtained: A_{iso} = 0.5 ± 0.2 MHz and T = 1.0 ± 0.5 MHz. The very small A_{iso} value indicates a nearly pure dipolar through-space interaction, which is characterized by a $1/r^3$ dependence on the electron-proton distance according to equation 2:

$$T = \frac{\mu_0}{4\pi} g_e g_n \beta_e \beta_n \frac{1}{r^3} \quad (2)$$

with *r* being the distance between the unpaired electron localized in the Ti^{3+} *d* orbitals and the ^1H nucleus. Using the experimental value obtained from the simulation the distance from the Ti^{3+} center and the proton can be estimated to be of the order of 0.43 nm.

3.3. The reductive activation of Ti ions in TS-1

The observation of Ti^{3+} framework ions upon reaction with TEA poses the question on how the initial Ti(IV) is reduced and what is the fate of the reaction products. We remark that this is a crucial question in the field of heterogeneous Ziegler-Natta catalysis, where these very same questions are at the center of a lively debate on the mechanism of activation-deactivation of the catalyst and still await to be answered.

The catalyst efficiency is known to change depending on the alkyl aluminium compound used as co-catalyst, as well as a function of the co-catalyst concentration. As far as the active sites are concerned, it is generally accepted that their formation proceeds by alkylation and reduction of the titanium species in the catalyst during the activation reaction with the co-catalyst [33,34]. In the case of classical Ziegler-Natta catalysts, the reduction of Ti (IV) to Ti^{3+} based on theoretical calculations is ascribed to the homolytic breaking of a Ti-Cl bond of $TiCl_4$ units adsorbed on $MgCl_2$ assisted by TEA. The driving force of the process is predicted to be the oxidative power of the liberated Cl atom, that attacks the Al center by nearly expelling one rather stable ethyl radical according to the following equation: $[Mg]/TiCl_4 + AlEt_3 \rightarrow [Mg]/TiCl_3\bullet + AlEt_3Cl\bullet$ [30]. This process is followed by transalkylation by TEA forming a Ti-C bond, which is considered the active catalytic species. Translating this mechanism to our case would imply in a first step the homolytic splitting of the Ti-O bond, followed by the alkylation of the Ti^{3+} species with formation of a $Ti\text{-}CH_2CH_3$ bond. Unfortunately due to the low natural abundance of ^{13}C (1.07%) we have no evidence of features amenable to the presence of ^{13}C from the HYSCORE spectra and specific experiments using ^{13}C enriched TEA will be needed to clarify the mechanism. However, some considerations can be made on the basis of observed proton coupling. The Ti^{3+}–H distance derived from the ^1H HYSCORE spectra (0.43 nm) seems incompatible with a σ-bonded alkyl unit. Considering a Ti-C bond length of the order of 0.205 nm and a C-H bond length of the order of 0.101 nm [35], a maximum Ti-H distance for a $Ti\text{-}CH_2R$ fragment can be estimated to be of the order of 0.3 nm, leading to a dipolar coupling of the order of T = 2.9 MHz, which is clearly incompatible with the experimental result. Indeed the ^1H hyperfine interaction was measured in the case of a Nickel-alkyl bond and a dipolar coupling of the order of 6 MHz was observed consistent with a Ni-H distance of the order of 0.21 nm in the $Ni\text{-}CH_2R$ fragment [36]. From these considerations the formation of a direct Ti-C bond seems implausible in our oxide based system. An alternative reaction pathway, accounting for the Ti reduction assisted by TEA, may be considered taking into account the formation of an alcoholate. In this way a charge transfer from the O^{2-} to the Ti^{4+} may be considered leading to a O^- Ti^{3+} intermediate, which would further react with TEA to give and adsorbed $[OCH_2CH_3]^-$ species, preserving the charge neutrality of the system. This hypothesis will need to be confirmed by ad hoc IR experiments. Regardless to the exact mechanism by which the Ti^{3+} tetrahedral species are formed, an important question is their chemical accessibility.

3.4. Coordination of ammonia through ^{14}N HYSCORE

In order to check for the reactivity of the formed Ti^{3+} species the coordination of ammonia to the formed Ti^{3+} centers was studied. As anticipated, upon delivering 20 mbar of ammonia a clear change in the CW-EPR spectrum is observed (Figure 1b), indicating a change in the local environment of the Ti^{3+} ions. Further insights into NH_3 coordination are obtained by means of HYSCORE experiments.

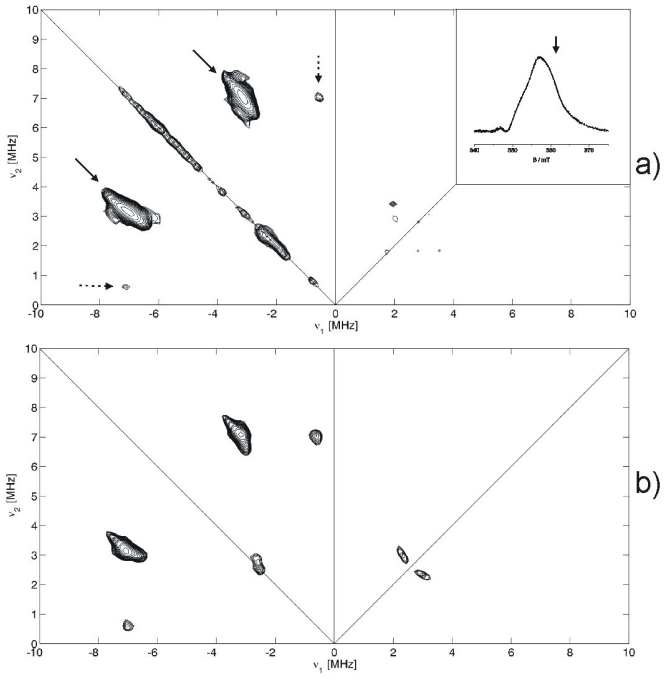

Figure 4. a) Experimental and b) simulated ^{14}N HYSCORE spectrum of reduced TS-1 contacted with NH_3 taken at the observer position 361.7 mT corresponding to the arrow in the inset (other positions are reported in Supporting Information) and τ= 172 ns. Solid arrows indicate ^{14}N double quantum transitions, while dotted arrows indicate single-double quantum transitions.

The HYSCORE spectrum of NH_3 adsorbed on the reduced TS-1 sample recorded at observer position 356.1 mT is reported in Figure 4 along with the corresponding computer simulation (in red). The spectrum is dominated in the (−, +) quadrant by a pair of cross-peaks centered at about (-3.5, 6.9) and (-6.9, 3.5) MHz, which are assigned to the double-quantum transitions (DQ) arising from the hyperfine interaction of the unpaired electron with a nitrogen nucleus (I = 1). The lack of combination peaks in the spectrum may be taken as an indication that only one single nitrogen is bound to the Ti^{3+} unit. This is in clear contrast with the case of tetrahedral Ti^{3+} species in the AlPO-5 matrix, where under even lower ammonia pressure evidence for two coordinated molecules was observed [26]. This preference towards 5-fold coordination in TS-1 is in agreement with recent valence to core-X-ray Emission Spectroscopy (vtc-XES) experiments corroborated by computational models [8].

Table 3. Spin-Hamiltonian parameters of $^{14}NH_3$ coordinated to various $3d^1$ transition metal ion centers. Hyperfine and quadrupole coupling constants are given in MHz.

System	(^{14}N) A_{iso}	(^{14}N) A_1	(^{14}N) A_2	(^{14}N) A_3	α, β, γ	e^2qQ/h	η	α, β, γ	Ref.
TS-1	4.6 ± 0.2	3.4 ± 0.2	4.6 ± 0.2	5.8 ± 0.2	0,80,20 ± 10	2.7 ± 0.2	0.1 ± 0.1	0,10,30 ± 10	This work
TiAlPO [a,b]	4.1 ± 0.2	3.5 ± 0.2	3.9 ± 0.2	4.8 ± 0.2	0,90,30	2.8	0.1	0,40,60	[26]
Ti(III) complex [c]	4.4 ± 0.2	3.5 ± 0.2	3.5 ± 0.2	6.2 ± 0.2	0,90 ± 20,0	2.3 ± 0.1	0.9 ± 0.1	-	[38]
VS-1-SBA [a]	4.6	4.4	4.6	4.86	0,30,0	2.5	0.5	-	[39]

[a] Two equivalent N nuclei. [b] In ref [26], the A_x and A_z value are inverted in the table. [c] [1-{2-(*t*-butyl)-2-sila-2,2-dimethyl}-2,3,4,5-tetramethylcyclopentadienyl]-methyl titanium (III) complex

The HYSCORE spectrum of a $S = 1/2$, $I = 1$ disordered system is typically dominated by the cross peaks between the DQ frequencies, whose position is related to hyperfine and quadrupole coupling terms [37]. In order to extract these parameters computer simulations of the HYSCORE spectrum (Figure 4), were performed and attention was paid to reproduce not only the shape of the DQ peaks, but also to fit the positions of the cross-peaks between the different single-quantum (SQ) frequencies and of the SQ–DQ cross-peaks (see arrows). The spin-Hamiltonian parameters extracted from the simulation are reported in Table 3.

The isotropic hyperfine coupling $|A_{iso}| = 4.6$ MHz derived from simulation, is similar, even though slightly higher, to that observed in the case of Ti^{3+} in the AlPO-5 matrix ($|A_{iso}| = 4.1$ MHz) and corresponds to a spin density population in the N 2*s* orbital ($a_0 = 1540$ MHz) [27] of 0.31%. This value is comparable to that observed for amino nitrogens axially ligated to Ti^{3+} in the [1-{2-(*t*-butyl)-2-sila-2,2-dimethyl}-2,3,4,5-tetramethylcyclopentadienyl]-methyl titanium (III) complex [38]. Similar values were also reported for coordination of ammonia to vanadyl sites of vanadium silicate-1 nanoparticles deposited in SBA-15 [39] and ZSM-5 zeolites [40] and are also comparable with values found for nitrogens equatorially bound to an oxovanadium cation, VO^{2+} [41], characterized by a d^1 ground state with the unpaired electron in the d_{xy} orbital.

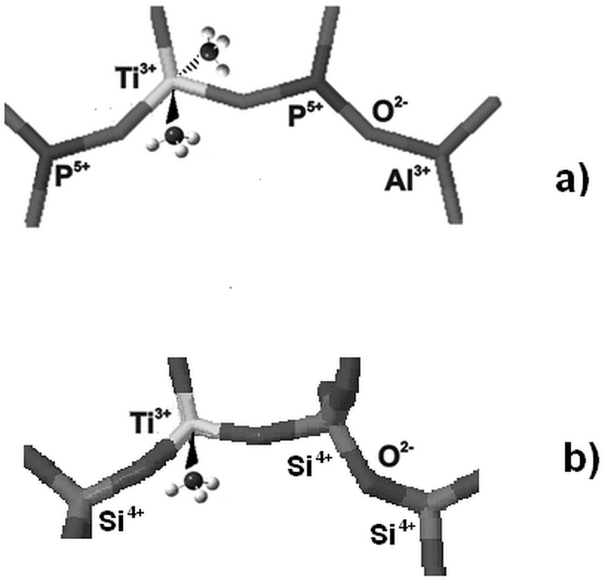

Scheme 1. NH_3 coordination in reduced Ti Silicalite-1 (a) and reduced TiAlPO (b).

The most intriguing fact that emerges from the ^{14}N HYSCORE spectra of adsorbed ammonia is the preference towards 5-fold coordination in TS-1 with respect to TiAlPO-5. The situation is schematically illustrated in Scheme 1. In the reduced TiAlPO-5 system, which also features tetrahedrally coordinated Ti^{3+} unambiguous evidence was obtained for the coordination of at least two ammonia molecules via the presence of distinct combination peaks in the ^{14}N HYSCORE spectrum [26]. Being the Ti^{3+} ions structurally equivalent, as also testified by the similarity of the g tensors extracted from the CW-EPR spectra, the difference in the chemical reactivity of the two species has to be found in the different nature of the two matrixes and in particular in their different bonding properties. Corà and Catlow [42] have shown by population and topological analyses of the calculated electronic density that the bonding in AlPOs is of molecular–ionic character and comprised of discrete Al^{3+} and PO_4^{3-} ions. On the other hand a continuum semicovalent network is the distinctive feature of the silica structure. The ionicity of the Al–O interaction compared to the covalent Si–O backbone may indeed explain the different behavior towards NH_3 ligation of the substituted Ti in the silicalite and AlPO frames. The coordination of two NH_3 molecules requires a pronounced rearrangement of the local framework structure, which indeed is relatively easy in the case of an ionic system. We remark that from the ^{31}P HYSCORE spectra we have conclusive evidence that the Ti^{3+} ion is replacing for an Al^{3+} sites, therefore the surrounding ionically bound PO_4^{3-} groups are expected to have enough flexibility to fulfill the Ti^{3+} tendency towards 6-fold coordination. On the other hand the rigid covalent structure of silicalite will hamper this structural rearrangement (bond angles will need to pass from approximately 109° to 90° degrees) allowing for the coordination of a single ammonia molecule. Indeed the ionic nature of AlPOs has been invoked to explain several different features of these solids including their hydrofilicity, however this is the first time that the bonding difference in the two matrixes can be directly linked to the different chemical reactivity of a isomorphously substituted TM ion.

Conclusion

The reaction of triethylaluminium with titanium silicalite TS-1, a zeotype material featuring isolated Ti^{4+} ions in tetrahedral coordination, was followed by means of CW-EPR and HYSCORE spectroscopies. The results provide evidence for the reducing power of triethylaluminium towards isolated Ti^{4+} ions through the formation of open-shell Ti^{3+} ions, whose framework nature is demonstrated by the combination of CW-EPR and ^{29}Si HYSCORE spectra. The chemical accessibility of such framework Ti^{3+} ions was probed against ammonia adsorption and evidence was found for preference of Ti^{3+} ions in TS-1 towards 5-fold coordination at variance with the case of tetrahedral Ti^{3+} in the framework of porous alumino-phosphate molecular sieves.

The implications of these results are manifold. From one side they provide a simple and effective route to generate accessible tetrahedrally coordinated open-shell Ti^{3+} sites in silica frames, which may open new and unexplored reaction pathways in coordination chemistry and redox catalysis, in particular considering recently reported highly accessible titanosilicates, such as large pore molecular sieves, mesoporous ordered materials, or layered-type zeolites [43] On the other hand this approach provides a robust framework to be extended to other oxide or halide based systems in the hope to achieve a more general understanding of the surface chemistry of alkylaluminum compounds and activation-deactivation mechanisms in heterogeneous Ziegler-Natta systems.

Experimental Section

Sample preparation

The TS-1 sample, made by ENI (Instituto G. Donegani, Novara, Italy) was fully characterized elsewhere.[2,3,8]. The Ti loading was 2.98 wt%, as determined by the cell volume expansion, and the absence of extra phases of TiO_2 was carefully checked [8].

For the spectroscopic characterization the calcined sample was loaded into a quartz tubular cell (Scheme 2) equipped with a 3 mm OD quartz tube allowing in situ EPR measurements and evacuated to a final pressure of 10^{-5} mbar at 673 K in order to obtain dehydrated samples. Triethylaluminium (TEA) (Aldrich) was purified by the freeze-pump-thaw method and delivered on the outgassed sample via the gas phase using the setup illustrated in Scheme 2. In order to prepare Ti^{3+}-ammonia complexes 20 mbar of ammonia were delivered on the activated sample at room temperature. For ESEEM measurements all samples were sealed, after checking the CW-EPR spectrum.

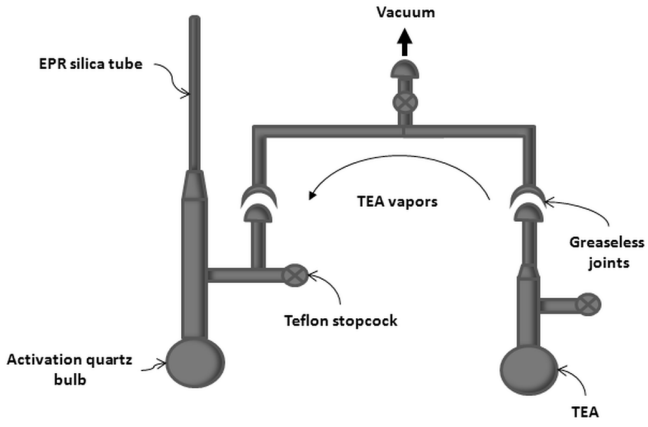

Scheme 2. Schematic representation of the experimental set-up used for the reductive activation of TS-1 with TEA vapors.

Spectroscopic characterization

X-band CW-EPR spectra were detected at 77 K on a Bruker EMX spectrometer (microwave frequency 9.75 GHz) equipped with a cylindrical cavity. A microwave power of 10 mW, modulation amplitude of 0.2 mT and a modulation frequency of 100 kHz were used. Pulse EPR experiments were performed on an ELEXYS 580 Bruker spectrometer (at the microwave frequency of 9.76 GHz) equipped with a liquid-helium cryostat from Oxford Inc. All experiments were performed at 10 K unless elsewhere stated. The magnetic field was measured by means of a Bruker ER035M NMR gaussmeter.

Electron-spin-echo (ESE) detected EPR experiments were carried out with the pulse sequence: $\pi/2 - \tau - \pi - \tau -$ echo, with microwave pulse lengths $t_{\pi/2}$ = 16 ns and t_{π} = 32 ns and a τ value of 200 ns.

Hyperfine Sublevel Correlation (HYSCORE) experiments [44] were carried out with the pulse sequence $\pi/2 - \tau - \pi/2 - t_1 - \pi - t_2 - \pi/2 - \tau -$ echo with the microwave pulse length $t_{\pi/2}$ = 16 ns and t_{π} = 16 ns. The time intervals t_1 and t_2 were varied in steps of 16 ns starting from 98 ns to 4898 ns. In order to avoid blind spot effects different τ values were chosen, which are specified in the figure captions. A four-step phase cycle was used for eliminating unwanted echoes. The time traces of the HYSCORE spectra were baseline corrected with a third-order polynomial, apodized with a Hamming window and zero filled. After two-dimensional Fourier transformation, the absolute value spectra were calculated. The spectra were added for the different τ values in order to eliminate blind-spot effects.

All spectra were simulated using the Easyspin package [45].

Acknowledgements

We gratefully acknowledge Prof. Silvia Bordiga for several useful comments and discussions. This work is part of the research program of the Dutch Polymer Institute (DPI), project nr. 754.

[1] a) M. Taramasso, G. Perego, B. Notari, *US Patent nr. 4410501*, **1983**; b) B. Notari, *Adv. Catal.* **1996**, *41*, 253-334.

[2] S. Bordiga, F. Bonino, A. Damin, C. Lamberti, *Phys. Chem. Chem. Phys.* **2007**, *9*, 4854-4878.

[3] G. Ricchiardi, A. Damin, S. Bordiga, C. Lamberti, G. Span, F. Rivetti, A. Zecchina, *J. Am. Chem. Soc.* **2001**, *123*, 11409-11419.

[4] a) C. Li, G. Xiong, Q. Xin, J. Liu, P. Ying, Z. Feng, J. Li, W. Yang, Y. Wang, G. Wang, X. Liu, M. Lin, X. Wang, E. Min, *Angew. Chem.* **1999**, *111*, 2358-2360; b) *Angew. Chem. Int. Ed.* **1999**, 38, 2220-2222.

[5] F. T. Fan, Z. C. Feng, C. Li, *Acc. Chem. Res.* **2010**, *43*, 378-387.

[6] A. Gamba, G. Tabacchi, E. Fois, *J. Phys. Chem. A* **2009**, *113*, 15006-15015.

[7] Q. Guo, K. Sun, Z. C. Feng, G. Li, G. Guo, F. T. Fan, C. Li, *Chem. Eur. J.* **2012**, *18*, 13854-13860.

[8] E. Gallo, F. Bonino, J. C. Swarbrick, T. Petrenko, A. Piovano, S. Bordiga, D. Gianolio, E. Groppo, F. Neese, C. Lamberti, P. Glatzel, *Chem. Phys. Chem.* **2013**, *14*, 79-83.

[9] A. M. Prakash, L. Kevan, *J. Catal.* **1998**, *178*, 586-597.

[10] C. K. Brozek, M. Dincă, *J. Am. Chem. Soc.* **2013**, *135*, 12886-12891.

[11] G. V. Oshovsky, B. Hessen, J. N. H. Reek, B. De Bruin, *Organometallics* **2011**, *30*, 6067-6070.

[12] T. D. Beeson, A. Mastracchio, J. B. Hong, K. Ashton, D. W. C. MacMillan, *Science* **2007**, *316*, 582-585.

[13] J. R. Severn, J. C. Chadwick, R. Duchateau, N. Friederichs, *Chem. Rev.* **2005**, *105*, 4073-4147.

[14] R. N. Kerber, A. Kermagoret, E. Callens, P. Florian, D. Massiot, A. Lesage, C. Copéret, F. Delbecq, X. Rozanska, P. Sautet, *J. Am. Chem. Soc.* **2012**, *134*, 6767-6775.

[15] E. A. Pidko, S. M. T. Almutairi, B. Mezari, P. C. M. M. Magusin, E. J. M. Hensen, *ACS Catal.* **2013**, *3*, 1504-1517.

[16] S. Maurelli, M. Vishnuvarthan, M. Chiesa, G. Berlier, S. Van Doorslaer, *J. Am. Chem. Soc.* **2011,** *133*, 7340-7343.

[17] M. B. Smith, *J. Phys. Chem.* **1967**, *71*, 364-370.

[18] A. M. Prakash, H. M. Sung-Suh, L. Kevan, *J. Phys. Chem. B* **1998**, *102*, 857-864.

[19] V. P. Solntsev, A. M. Yurkin, *Cryst. Reports* **2000**, *45*, 128-132.

[20] A. Abraham, B. Bleaney, in *Electron Paramagnetic Resonance of Transition Ions*, Oxford University Press, Oxford, **1970**.

[21] M. L. Du, C. Rudowicz, *Phys. Rev. B* **1992**, *46*, 8974.8977.

[22] M. Yang, W. Xiao-Xuan, Z. Wen-Chen, *Radiat. Eff. Defect S.* **2008**, *163*, 79-83.

[23] J. A. Weil, J. R. Bolton, J. E. Wertz, in *Electron Paramagnetic Resonance: Elementary Theory and Practical Applications*, John Wiley & Sons, New York, **1994**.

[24] J. S. Griffith, in *The Theory of Transition-Metal Ions,* Cambridge University Press, Cambridge, **1964**.

[25] B. N. Figgis, in *Introduction to Ligand Fields*, John Wiley & Sons, New York, **1967**.

[26] S. Maurelli, M. Vishnuvarthan, G. Berlier, M. Chiesa, *Phys. Chem. Chem. Phys.* **2012**, *14*, 987–995

[27] S. Zamani, V. Meynen, A. M. Hanu, M. Mertens, E. Popovici, S. Van Doorslaer, P. Cool, *Phys. Chem. Chem. Phys*. **2009**, *11*, 5823-5832.

[28] J. A. J. Fitzpatrick, F. R. Manby, C. M. Western, *J. Chem. Phys*. **2005**, *122*, 084312-1-12.

[29] S. A. Dikanov, B. D. Liboiron, C. Orvig, *J. Am. Chem. Soc*. **2002**, *124*, 2969-2978.

[30] G. N. Vayssilov,*Catal. Rev.* **1997**, *39*, 209-251.

[31] D. Arieli, D. E. W. Vaughan, K. G. Strohmaier, D. Goldfarb *J. Am. Chem. Soc.* **1999**, *121*, 6028 -6032.

[32] D. Goldfarb, *Phys. Chem. Chem. Phys*. **2006**, *8*, 2325-2343.

[33] H. Mori, K. Hasebe, M. Terano, *Polymer* **1999**, *40*, 1389-1394.

[34] N. Bahri-Laleh, A. Correa, S. Mehdipour-Ataei, H. Arabi, M. Nekoomanesh-Haghighi, G. Zohuri, L. Cavallo, *Macromol*. **2011**, *44*, 778-783.

[35] M. K. Skalli, A. Markovits, C. Minot, A. Belmajdoub, *Catal. Lett.* **2001**, *76*, 7-9.

[36] D. Hinderberger, R. P. Piskorski, M. Goenrich, R. K. Thauer, A. Schweiger, J. Harmer, B. Jaun, *Angew. Chem*. **2006**, *118*, 3684-3689.

[37] S. A. Dikanov, Y. D. Tsvetkov, M. K. Bowman, A. V. Astashkin, *Chem. Phys. Lett.* **1982**, *90*, 149-153.

[38] S. Van Doorslaer, J. J. Shane, S. Stoll, A. Schweiger, M. Kranenburg, R. J. Meier, *J. Organomet. Chem*. **2001**, *634*, 185-192.

[39] S. Zamani, M. Chiesa, V. Meynen, Y. Xiao, B. Prélot, J. Zajac, F. Verpoort, P. Cool, S. Van Doorslaer, *J. Phys. Chem. C* **2010**, *114,* 12966-12975.

[40] J. Woodworth, M. K. Bowman, S. C. Larsen, *J. Phys. Chem. B* **2004**, *108*, 16128-16134.

[41] a) K. Fukui, H. Ohya-Nishigchi, H. Kamada, *Inorg. Chem.* **1997**, *36*, 5518-5529; b) C. Buy, T. Matsui, S. Andrianambinintsoa, C. Sigalat, G. Girault, J. L. Zimmermann, *Biochemistry* **1996**, *35*, 14281-14293; c) K. Fukui, H. Ohya-Nishigchi, H. Kamada, M. Iwaizumi, Y. Xu, *Bull. Chem. Soc. Jpn.* **1998**, *71*, 2787-2796; d) S. A. Dikanov, A. M. Tyryshkin, J. Hüttermann, R. Bogumil, H. Witzel, *J. Am. Chem. Soc.* **1995**, *117*, 4976-4986; e) S. A. Dikanov, R. I. Samoilova, J. A. Smieja, M. K. Bowman, *J. Am. Chem. Soc.* **1995**, *117*, 10579-10580; f) C. F. Mulks, B. Kirste, H. Van Willigen, M. K. Bowman, *J. Am. Chem. Soc.* **1982**, *104*, 5906-5911; g) B. Kirste, H. Van Willigen, *J. Phys. Chem.* **1982**, *86*, 2743-2753.

[42] F. Corà, C. R. A. Catlow, *J. Phys. Chem. B* **2001**, *105*, 10278-10281.

[43] M. Moliner, A. Corma, Micropor. Mesopor. Mater. **2013**, http://dx.doi.org/10.1016/j.micromeso.2013.08.003.

Probing the Redox Chemistry of Ti Silicalite-1.

Formation of Tetrahedral Ti^{3+} Centers by Reaction with Triethylaluminium.

Elena Morra, Elio Giamello, Mario Chiesa*.

Department of Chemistry, University of Torino Via Giuria, 7 - 10125 Torino, Italy
Dutch Polymer Institute (DPI), P.O. Box 902, 5600 AX Eindhoven, The Netherlands

Supporting material

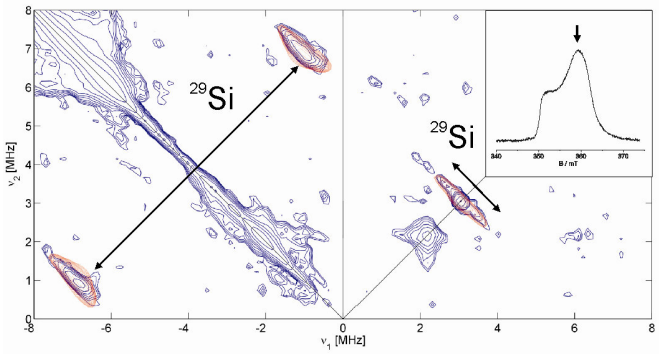

Figure S1. Experimental (blue) and simulated (red) ^{29}Si HYSCORE spectra of reduced TS-1 taken at observer position 359.5 mT corresponding to the arrow in the inset . Two τ *values* (192 ns and 224 ns) are summed together after Fourier transform in both the experimental and simulated spectra. The simulation was performed considering a three spin system (S=1/2, I=1/2, I=1/2).

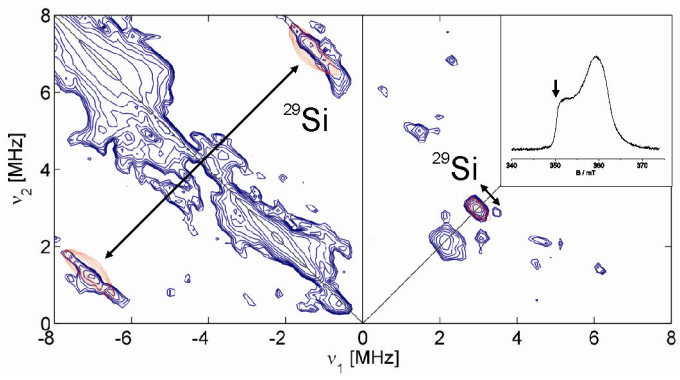

Figure S2 Experimental (blue) and simulated (red) ^{29}Si HYSCORE spectra of reduced TS-1 taken at observer position 350.2 mT corresponding to the arrow in the inset. The spectrum was recorded at τ=192 ns.

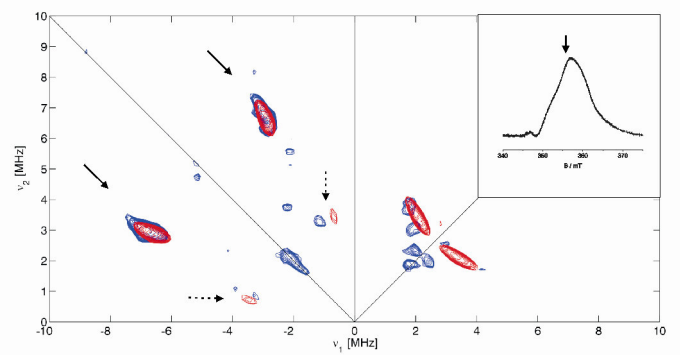

Figure S3 Experimental (blue) and simulated (red) ^{14}N HYSCORE spectrum of reduced TS-1 contacted with NH_3 taken at the observer position 356.1 mT corresponding to the arrow in the inset. Solid arrows indicate ^{14}N double quantum transitions, while dotted arrows indicate single quantum transitions. The spectrum was recorded at τ=172 ns

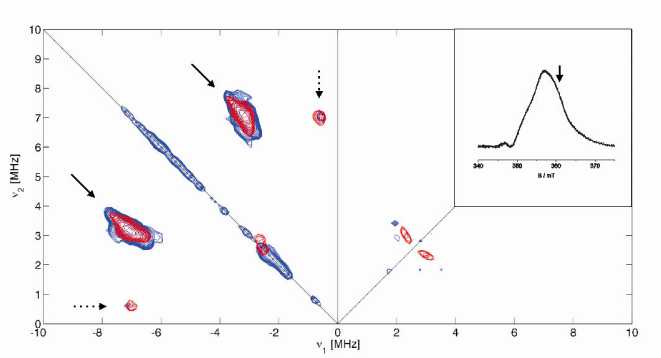

Figure S4. Experimental (blue) and simulated (red) ^{14}N HYSCORE spectrum of reduced TS-1 contacted with NH_3 taken at the observer position 361.7 mT corresponding to the arrow in the inset and τ= 172 ns. Solid arrows indicate 14N double quantum transitions, while dotted arrows indicate single-double quantum transitions.